International Journal of Electrical, Electronic and Communication Sciences
ISSN: 2517-9438
Vol:4, No:6, 2010

Sensorless Control of Induction Motor:Design and Stability Analysis

Nadia Bensiali, Erik Etien, Amar Omeiri and Gerard Champenois

Abstract—Adaptive observers used in sensorless control of induction motors suffer from instability especally in regenerating mode. In this paper, an optimal feed back gain design is proposed, it can reduce the instability region in the torque speed plane .

Keywords—Induction motor drive, adaptive observer, regenerating mode, stabilizing design.

I. Introduction

During the last decade, there has been a considerable interest in studying stability of adaptive observers used in sensorless control of induction motors. This is mainly due to their economical benefit and fragility of mechanical sensors and also the difficulty of installing this type of sensor in many applications. These systems suffer from instability problems and sensitivity to parameter mismatch at low speed operation. The sensorless systems require estimation of internal state variables of the machine such as speed and rotor flux from input variables like stator voltage and stator current [1] [3] .

Many works were led in order to eliminate or to reduce unstable regions.They acts on:

- speed adaptation law [6]
- feedback gain [4], [7],
- speed adaptation law and feedback gain simultaneously [2].

In this paper, first, stability of induction motor alone is done and second the design of a feed back gain that minimizes the unstability regions in the torque-speed plane to a straight line corresponding to DC excitation is described.

II. Controller design

The four parameter induction motor model using complex notations is described in the synchronous rotating reference frame by the following equations :

$$\begin{cases} \frac{d}{dt}\underline{\psi}_R = -(\frac{1}{\tau_r} + j\omega_{sl})\underline{\psi}_R + R_R\underline{i}_s \\ \frac{d}{dt}\underline{i}_s = \frac{1}{L_\sigma}(\frac{1}{\tau_r} - j\omega)\underline{\psi}_R - (\frac{1}{\tau_\sigma} + j\omega_s)\underline{i}_s + \frac{1}{L_\sigma}\underline{u}_s \\ \frac{d\omega}{dt} = \frac{p^2}{J}\Im(\underline{i}_s\psi_R^*) \end{cases} \quad (1)$$

With :$\tau_\sigma = \dfrac{L_\sigma}{R_R + R_s}$ and $\tau_r = \dfrac{L_M}{R_R}$.

$i_s = i_{sd} + ji_{sq}$ stator current space vector
$\psi_R = \psi_{rd} + j\psi_{rq}$ Rotor flux space vector
ψ_{ref} Rotor flux reference
ω_{sl} slip frequency
ω electrical rotor speed
R_s, R_R Stator and Rotor resistance
L_M, L_σ Magnetizing and Leakage inductance

A. Stability analysis of induction motor

Stability analysis of induction motor alone can be studied by linearizing system (1) around an equilibrium operating point [5]. the obtained system is :

$$\begin{cases} \frac{d}{dt}\delta\psi_{Rd} = -\frac{1}{\tau_r}\delta\psi_{Rd} + \omega_{slo}\delta\psi_{Rq} + R_R\delta i_{sd} \\ \frac{d}{dt}\delta\psi_{Rq} = -\omega_{slo}\delta\psi_{Rd} - \frac{1}{\tau_r}\delta\psi_{Rq} + R_R\delta i_{sq} - \psi_{Ro}\delta\omega_{sl} \\ \frac{d}{dt}\delta i_{sd} = \frac{1}{L_\sigma\tau_r}\delta\psi_{Rd} + \frac{\omega}{L_\sigma}\delta\psi_{Rq} - \frac{1}{\tau_\sigma}\delta i_{sd} + \omega_s\delta i_{sq} + \\ \delta\omega_s i_{sqo} + \frac{1}{L_\sigma}u_{sd} \\ \frac{d}{dt}\delta i_{sq} = -\frac{\omega}{L_\sigma}\delta\psi_{Rd} + \frac{1}{L_\sigma\tau_r}\delta\psi_{Rq} - \omega_s\delta i_{sd} - \frac{1}{\tau_\sigma}\delta i_{sq} \\ -\frac{1}{L_\sigma}\psi_{Ro}\delta\omega - \delta\omega_s i_{sdo} + \frac{1}{L_\sigma}u_{sq} \\ \frac{d}{dt}\delta\omega = \frac{p^2}{J}(i_{sqo}\delta\psi_{Rd} - i_{sdo}\delta\psi_{Rq} + \psi_{Ro}\delta i_{sq}) \end{cases} \quad (2)$$

With : $\delta\psi_{Rd} + j\delta\psi_{Rq} = \delta\psi_R$, $\delta i_{sd} + j\delta i_{sq} = \delta i_s$

The state matrix corresponding to the state vector $\delta x = [\ \delta\psi_{Rd} \quad \delta\psi_{Rq} \quad \delta i_{sd} \quad \delta i_{sq} \quad \delta\omega\ ]^T$ is:

$$A_o = \frac{1}{\tau_r}\begin{bmatrix} -1 & \omega_{sl} & L_M & 0 & 0 \\ -\omega_{sl} & -1 & 0 & L_M & \tau_r\psi_{Ro} \\ \frac{1}{L_\sigma} & \frac{\tau_r\omega_{so} - \omega_{sl}}{L_\sigma} & -\frac{\tau_r}{\tau_\sigma} & \tau_r\omega_{so} & 0 \\ -\frac{\tau_r\omega_{so} - \omega_{sl}}{L_\sigma} & \frac{1}{L_\sigma} & -\tau_r\omega_{so} & -\frac{\tau_r}{\tau_\sigma} & -\frac{\tau_r}{L_\sigma}\psi_{Ro} \\ \frac{p^2\psi_{Ro}\omega_{sl}}{JR_R} & -\frac{p^2\psi_{Ro}}{JR_R} & 0 & \frac{p^2\tau_r}{J}\psi_{Ro} & 0 \end{bmatrix} \quad (3)$$

With: $\omega_{sl} = \tau_r\omega_{slo}$

Ploting unstable eigen values (E.V) of the state matrix A_o permit localization of unstable regions in the torque speed plane as shown on figure (1) .

Note that the line (D_1) is known as the unobsrvability line obtained in the case of DC excitation ($\omega_{so} = 0$).

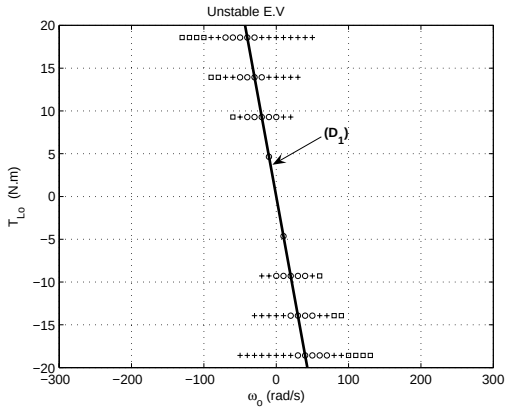

Fig. 1. Unstable E.V in the plan $\{\omega_o, T_{Lo}\}$

B. Analytical expression of IM unstable regions

In order to establish analytical expression of stability limits, the following property is used

$$det(A_o) = \prod_{i=1}^{5} \lambda_i \tag{4}$$

where λ_i are the eigen values of matrix A_o. the system stability implies that the five eigen values must have a negative real part. Consequently, a condition of stability for system (3) is

$$det(A_o) < 0. \tag{5}$$

The limit of stability is done by $det(A_o) = 0$. Using Mapple/Matlab and without any simplification, the expression find is

$$det(A_o) = \frac{p^2 \psi_{Ro}}{\tau_r^2 R_R J L_\sigma^2} \left[\omega_{sl}^2 \left(R_s^2 + (L_\sigma \omega_{so})^2\right) - \left(R_s^2 + (L_s \omega_{so})^2\right)\right] \tag{6}$$

so:

$$\omega_{slo} = \pm \frac{1}{\tau_r} \sqrt{\frac{R_s^2 + (L_s \omega_{so})^2}{R_s^2 + (L_\sigma \omega_{so})^2}}$$

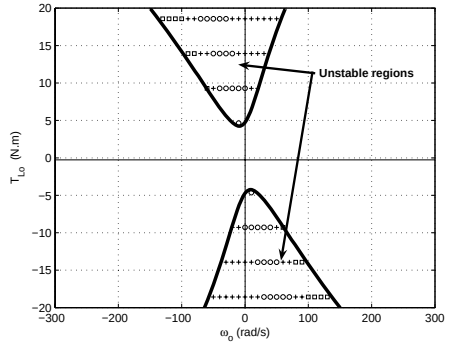

Fig. 2. Stability limits in the angular speed/torque plane

These conditions of stability are represented in the torque/velocity plane by figure (2) . It can be verified that unstable regions are the same as obtained previously with eigen values.

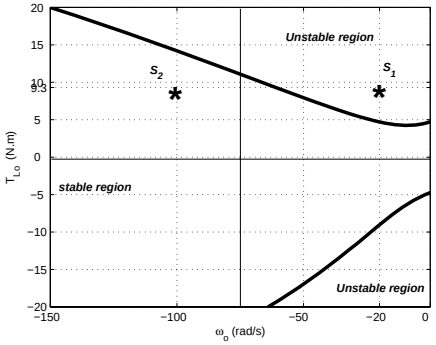

Fig. 3. Operating points

Fig. 4 and 5 show tries in quadrant I and II under load torque $T_{Lo} = 9.3N.m$, for tow operating points s_1 and s_2 ,localized respectively in unstable and stable regions (figure 3).

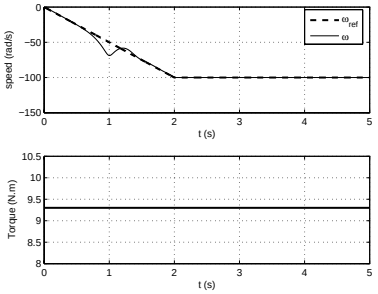

Fig. 4. Tries in stable region (quadrant II): actual velocity (solid line), reference velocity (dashed line). $\omega_{ref} = -100rad/s$, load torque $T_{Lo} = 9.3N.m$

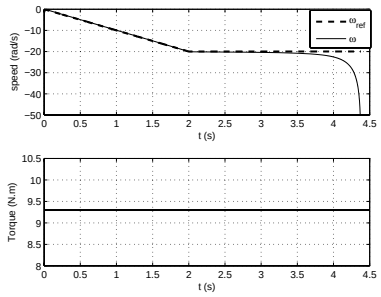

Fig. 5. Tries in unstable region (quadrant II): actual velocity (solid line), reference velocity (dashed line). $\omega_{ref} = -20rad/s$, load torque $T_{Lo} = 9.3N.m$

III. Observer design

The conventional full-order observer is defined by

$$\begin{cases} \frac{d}{dt}\underline{\widehat{\psi}}_R = -(\frac{1}{\tau_r} + j\widehat{\omega}_{sl})\underline{\widehat{\psi}}_R + R_R\underline{\widehat{i}}_s + G_r\underline{e}_i \\ \frac{d}{dt}\underline{\widehat{i}}_s = \frac{1}{L_\sigma}(\frac{1}{\tau_r} - j\widehat{\omega})\underline{\widehat{\psi}}_R - (\frac{1}{\tau_\sigma} + j\widehat{\omega}_s)\underline{\widehat{i}}_s + \frac{1}{L_\sigma}\underline{u}_s + G_s\underline{e}_i \\ \frac{d\widehat{\omega}}{dt} = -K_{i\omega}\epsilon - K_{p\omega}\frac{d}{dt}\epsilon,\ \epsilon = \Im\left\{e^{-j\phi}e_i\widehat{\psi}_R^*\right\} \end{cases} \tag{7}$$

with:

$$e^{-j\phi} = cos\phi - jsin\phi \tag{8}$$

$$G_r = \begin{bmatrix} g_{rd} & -g_{rq} \\ g_{rq} & g_{rd} \end{bmatrix},\ G_s = \begin{bmatrix} g_{sd} & -g_{sq} \\ g_{sq} & g_{sd} \end{bmatrix}$$

System obtained by linearizing observer model (7), and for $\phi = 0$,is:

$$\begin{cases} \frac{d}{dt}\delta\widehat{\psi}_{Rd} = -\frac{1}{\tau_r}\delta\widehat{\psi}_{Rd} + \widehat{\omega}_{slo}\delta\widehat{\psi}_{Rq} + R_R\delta\widehat{i}_{sd} \\ \frac{d}{dt}\delta\widehat{\psi}_{Rq} = -\widehat{\omega}_{slo}\delta\widehat{\psi}_{Rd} - \frac{1}{\tau_r}\delta\widehat{\psi}_{Rq} + R_R\delta\widehat{i}_{sq} \\ -\psi_{ref}\delta\widehat{\omega}_{sl} \\ \frac{d}{dt}\delta\widehat{i}_{sd} = \frac{1}{L_\sigma\tau_r}\delta\widehat{\psi}_{Rd} + \frac{\widehat{\omega}_o}{L_\sigma}\delta\widehat{\psi}_{Rq} - \frac{1}{\tau_\sigma}\delta\widehat{i}_{sd} \\ +\widehat{\omega}_{so}\delta\widehat{i}_{sq} + \delta\widehat{\omega}_{so}\widehat{i}_{sqo} + \frac{1}{L_\sigma}u_{sd} \\ \frac{d}{dt}\delta\widehat{i}_{sq} = -\frac{\widehat{\omega}_o}{L_\sigma}\delta\widehat{\psi}_{Rd} + \frac{1}{L_\sigma\tau_r}\delta\widehat{\psi}_{Rq} - \widehat{\omega}_{so}\delta\widehat{i}_{sd} \\ -\frac{1}{\tau_\sigma}\delta\widehat{i}_{sq} - \frac{1}{L_\sigma}\widehat{\psi}_{ref}\delta\widehat{\omega}_o - \delta\widehat{\omega}_{so}\widehat{i}_{sdo} + \frac{1}{L_\sigma}u_{sq} \\ \frac{d}{dt}\delta\widehat{\omega} = -K_{i\omega}\psi_{ref}\delta e_{iq} - K_{p\omega}\psi_{ref}(-\omega_{so}\delta e_{id} - \frac{1}{\tau_\sigma}\delta e_{iq} - \frac{\omega_o}{L_\sigma}\delta e_{\psi d} \\ +\frac{1}{L_\sigma\tau_r}\delta e_{\psi q} - \frac{1}{L_\sigma}\psi_{ref}\delta e_\omega) \end{cases} \tag{9}$$

with: $e_{ido} = i_{sdo} - \widehat{i}_{sdo}$, $e_{iqo} = i_{sqo} - \widehat{i}_{sqo}$,

IV. Global stability analysis

A new state vector δe is defined with :$\delta e = \begin{bmatrix} \delta e_{\psi d} & \delta e_{\psi q} & \delta e_{id} & \delta e_{iq} & \delta e_\omega \end{bmatrix}$.

The state matrix describing the estimation error is :

$$\widehat{A}_1 = \begin{bmatrix} -\frac{1}{\tau_r} & \omega_{slo} & R_R - g_{rd} & g_{rq} & 0 \\ -\omega_{slo} & -\frac{1}{\tau_r} & -g_{rq} & R_R - g_{rd} & \psi_{ref} \\ \frac{1}{L_\sigma\tau_r} & \frac{\omega_o}{L_\sigma} & -\frac{1}{\tau_\sigma} - g_{sd} & \omega_{so} + g_{sq} & 0 \\ -\frac{\omega_o}{L_\sigma} & \frac{1}{L_\sigma\tau_r} & -\omega_{so} - g_{sq} & -\frac{1}{\tau_\sigma} - g_{sd} & -\frac{1}{L_\sigma}\psi_{ref} \\ \widehat{A}_1(51) & \widehat{A}_1(52) & \widehat{A}_1(53) & \widehat{A}_1(54) & \widehat{A}_1(55) \end{bmatrix} \tag{10}$$

with:

$\widehat{A}_1(51) = -K_{p\omega}\omega_{so}\psi_{ref}$,

$\widehat{A}_1(52) = (K_{i\omega} - \frac{K_{p\omega}}{\tau_\sigma})\psi_{ref}$

$\widehat{A}_1(53) = \frac{-K_{p\omega}\omega_o\psi_{ref}}{L_\sigma}$

$\widehat{A}_1(54) = \frac{K_{p\omega}\psi_{ref}}{L_\sigma\tau_r}$

$\widehat{A}_1(55) = \frac{-K_{p\omega}\psi_{ref}^2}{L_\sigma}$

To locate unstable zones, a representation of poles which have a positive real part is proposed . Figure (6) shows these zones for $K_{i\omega} = 3000$, and different $K_{p\omega}$.

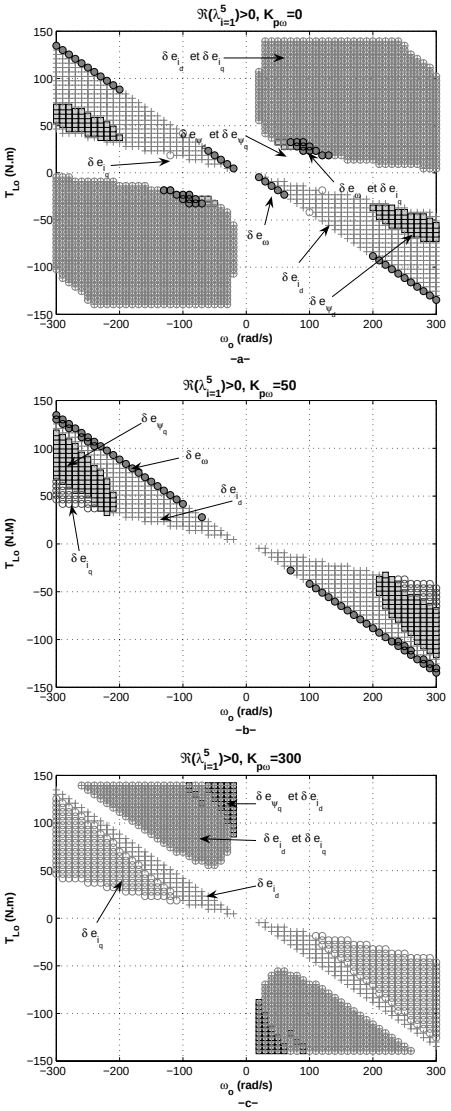

Fig. 6. Unstable zones for $K_{i\omega} = 3000$, and different $K_{p\omega}$

These figures show that unstable poles apeare in both monitoring and regenerating modes. For $K_{p\omega} = 50$ unstable zones in monitoring mode are eliminated.
Criterion of determinant is used to find analytical expression of these regions in torque-speed plane . It gives:

$$\begin{cases} T_{Lo} = -p\frac{\psi_{ref}^2}{R_R}\omega_o & (D_1) \\ T_{Lo} = -p\frac{\psi_{ref}^2}{R_R}(\frac{L_\sigma + L_M}{\tau_r R_s + L_\sigma + L_M})\omega_o & (D_2) \end{cases} \tag{11}$$

These tow lines (figure 7)define the limits of unstable regions in regenerating mode whatever is $K_{p\omega}$.

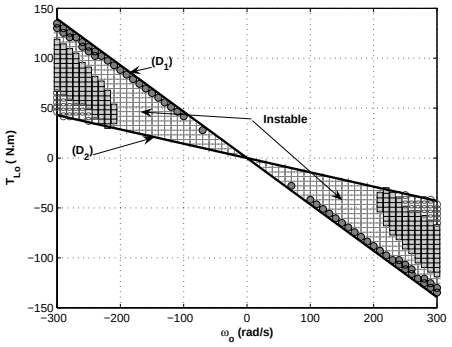

Fig. 7. Unstable zones in regenerating mode

To validate these results, in figure (8) ,simulations are done when the induction motor is operating in regenerating mode. It is clear that as soon as the motor run across the boundary into the predicted unstable region, the sensorless system becomes unstable.

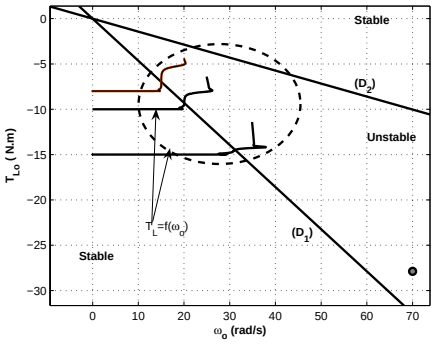

Fig. 8. Simulation results showing unstable region in torque speed plane

Figures (9 a, b) illustrate simulation results for speed reverse under nominal torque $T_{Lo} = 7N.m$ and load torque $T_{Lo} = -10N.m$ respectively .

Results show that in regenerating modes (quadrant II and IV in torque speed plane) divergence is highlighted between real and estimate variables.

Stability of observers employed in sensorless control of induction motor is not ensured. The drives dynamic performance and the estimators tracking capability are strongly affected. Solution to this problem is to find an optimal feedback gain which can reduce or eliminate unstable zones.

V. Optimal gain design

The principle of the optimal unstability reduction proposed here consists in the calculation of the feedback gain imposing the condition

$$(D_1) = (D_2) \tag{12}$$

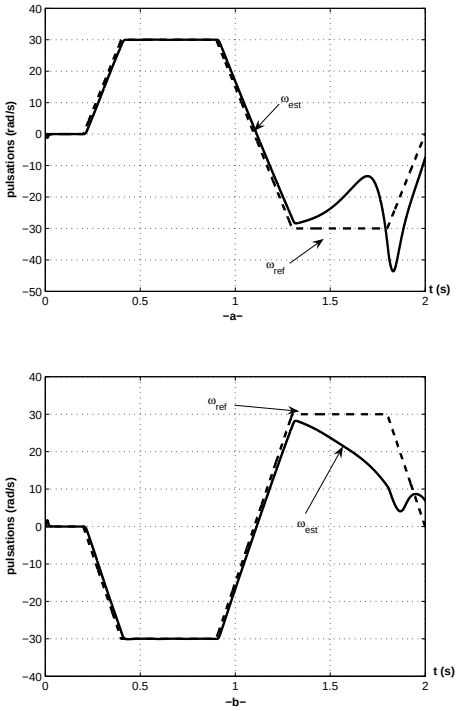

Fig. 9. Reversal speed trajectory from stable to unstable region:(a)$T_{Lo} = 7N.m$,(b) $T_{Lo} = -10N.m$

More precisely, a feed back gain superposing (D_2) with (D_1), must be calculated. Then, the unstable region will be limited to the line (D_1) (Fig. 10). It can be noted that, whatever the structure of the matrix G, (D_1) is always defined by $\omega_{so} = 0$.

In this case the determiant may be expressed as:

$$det(\widehat{A}_1) = \alpha\omega_{so}^2 \tag{13}$$

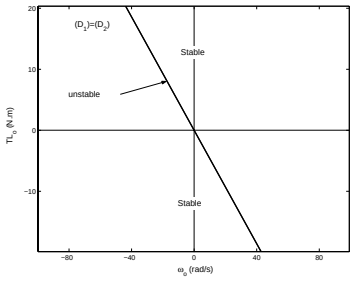

Fig. 10. Optimal unstability region limited to the line (D_1)

The particular forms $G_r = 0$ and $G_s = \begin{bmatrix} g_{sd} & 0 \\ 0 & g_{sd} \end{bmatrix}$ are choosen

This gives:

$$det(\widehat{A}_1) = -\frac{k_{i\omega}\psi_{ref}^2\omega_{so}}{L_\sigma\tau_s} \left[\omega_{so}(1+\frac{\tau_s}{\tau_r}+g_{sd}\tau_s) - \omega_o(1+\tau_s g_{sd}-\frac{R_R}{R_R+R_s})\right] \quad (14)$$

To obtain form expressed by (13), we choose:

$$g_{sd} = -\frac{R_s}{L_\sigma} \quad (15)$$

In order to validate the proposed design, simulations results are presented. In Fig. 11, the operating point is brought in the vicinity of (D_1). This show that the unstability region is considerably reduced by the proposed gain design.

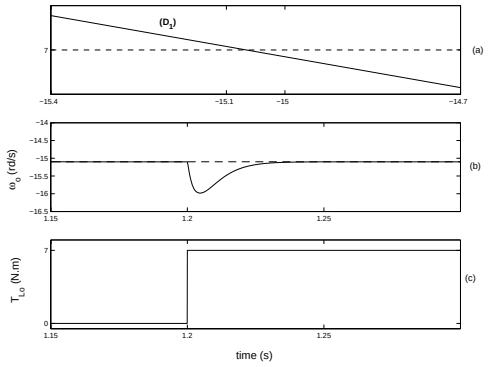

Fig. 11. Velocity transient in the vicinity of (D_1) in regenerating mode (quadrant 2) (a), from $T_{Lo} = 0\ N.m$ to $T_{Lo} = 7\ N.m$ (c), low velocity ($\omega_o = 15,1 rd/s$) (b), $K_i = 3000$, $K_p = 300$.

Fig. 12 shows simulation results for tries at constant nominal torque in renerating mode. The operating point trajectory cross the line (D_1) without unstability.

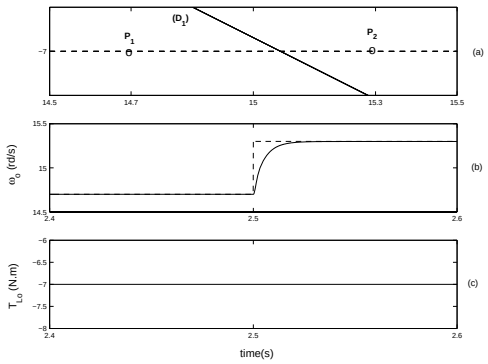

Fig. 12. Stable velocity transient crossing (D_1), from P_1 to P_2, in regenerating mode (quadrant 4) (a), from $\omega_o = 14.7\ rad/s$ to $\omega_o = 15.3\ rad/s$ (b), nominal torque ($T_{Lo} = -7N.m$) (c), $K_i = 3000$, $K_p = 300$.

Fig. 13 illustrates simulation results for speed reverse under nominal torque . this figure shows that there is no loose of control, and estimator tracking capability is garanteed.

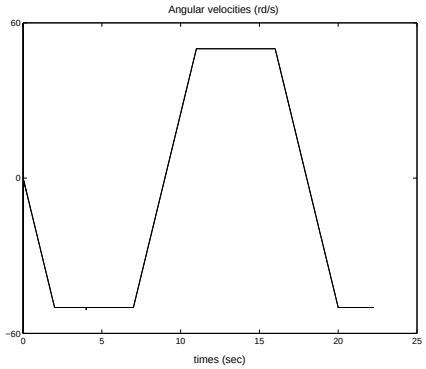

Fig. 13. Actual velocity (solid line), reference velocity (dashed line). Transition from stable to stable region crossing the line of unstability (D_1)

VI. Conclusion

In this paper,stability of the speed sensorless vector control of induction motors is analysed. This allows to design an optimal feed back gain which can reduce the unstable zones to a line defined by DC excitation when all parameters are known. The gain obtained depend on motor parameters. These parameters change during motor operation due to temperature rise. Perspectives proposed is to study the stability of an extended adaptive observer which estimates rotor speed and stator resistance simultaneously.

References

[1] C. Chaigne, E. Etien, S. Cauet, L. Rambault,*Commande vectorielle sans capteur des machines asynchrones.* ,Hermes science, Lavoisier, 2005.
[2] M. Hinkkanen, *Stabilisation of Regenerating-Mode Operation in Sensorless Induction Motor Drives by Full-Order Flux Observer Design,IEEE Transactions on Industrial Electronics,vol. 51, n^o* 6 2004.
[3] H. Kubota and K. Matsuse, *DSP-Based Speed Adaptive Flux Observer of Induction Motor*, *IEEE Transactions on industry Applications,vol. 29, n^o* 2,1993.
[4] H. Kubota and I. Sato, *Regeneratin-Mode Low-Speed Operation of Sensorless Induction Motor Drive With Adaptive Observer*, *IEEE Transactions on industry Applications,vol. 38, n^o* 4,2002.
[5] F. Morand, *Technique s d'Obsrvation sans capteur de Vitesse en vue de la Commande des Machines Asynchrone*, Phd Thesis *Institut National des Sciences appliquées de Lyon*, , 2005.
[6] M. Rashed and F. Stronach and P. Vas, *A stable MRAS-based sensorless vector control induction motor drive at low speeds*, *in Conf. Rec. IEEE IEMDC*, 2003.
[7] S. Suwankawin and S. Sangwongwanich, *A Speed-Sensorless IM Drive With Decoupling Control and Stability Analysis of Speed Estimation*, *IEEE Transactions on industrial electronics,vol. 49, n^o* 2, 2002.

Nadia Bensiali N. Bensiali is with the department of power electronics, institute of electrical engineering, Badji Mokhtar university, Annaba Algeria. e-mail:(bensialin@yahoo.fr). Her major field of research is the sensor-less control of induction motor,power electronics.

Erik Etien E. Etien is with Laboratory of Automatic and Industrial Informatic laboratory of Poitiers, France.His research interests induction motor observers in low speed functioning and identification of non-linear magnetic models.e-mail(erik.etien@univ-poitiers.fr)

Amar Omeiri A. Omeiri is PHD in the University of Badji Mokhtar Annaba Algeria. His field of research, is control of electrical machines, power electronics and energy quality.

Gerard Champenois G. Champenois is professor at the University of Poitiers (France). His major fields of research are electrical machines associated with static converter, control, modelling and diagnosis by parameter identification techniques.